Research in Astronomy and Astrophysics, 24:085011 (8pp), 2024 August https://doi.org/10.1088/1674-4527/ad621e

The Astrometric Performance of the China Space Station Telescope (CSST) Sky Survey in Extending the Gaia Celestial Reference Frame

Jun Yao[1], Jia-Cheng Liu[1], Niu Liu[1], Zi Zhu[1,2], and Zhen-Wei Wang[1]
[1] School of Astronomy and Space Science, Key Laboratory of Modern Astronomy and Astrophysics (Ministry of Education), Nanjing University, Nanjing 210023, China; jcliu@nju.edu.cn
[2] University of Chinese Academy of Sciences, Nanjing 211135, China
Received 2024 April 1; revised 2024 June 19; accepted 2024 July 10; published 2024 July 31

Abstract

The multi-color imaging sky survey conducted by the China Space Station Telescope (CSST) holds significant promise for advancing the development of the celestial reference frame. In this study, we focus on assessing the astrometric performance of the CSST celestial reference frame (CSST-CRF) in extending the Gaia Celestial Reference Frame 3 (Gaia-CRF3). First, the orientation precision of the CSST reference frame is evaluated using a simulated set of extragalactic sources with CSST g magnitudes ranging from 18 to 25 mag. The estimated orientation uncertainty caused by random error insignificantly affects the alignment between Gaia-CRF3 and the CSST-CRF. Then, the systematic effect of incomplete CSST sky coverage on the alignment between CSST-CRF and Gaia-CRF3 is discussed by analyzing the differences between the subset of Gaia-CRF3 in the CSST observation region (Gaia-CRF3′) and Gaia-CRF3 as a whole. Using the third International Celestial Reference Frame (ICRF3) S/X band as an intermediate reference frame, the orientation offset between Gaia-CRF3′ and Gaia-CRF3 is estimated to be 20 μas. This offset is marginally larger than the orientation offset between Gaia-CRF3 and the ICRF3, approximately 15 μas. The residual spin and glide rate of Gaia-CRF3′ are derived from the proper motions, consistent with that of Gaia-CRF3 within the formal error. Finally, we explore the role of CSST in establishing a multi-band celestial reference frame by comparing its limiting magnitude and observation accuracy with existing catalogs in the infrared and ultraviolet bands. Thanks to its broad wavelength coverage and high-precision measurements, CSST is well-positioned to make significant contributions to the development of a multi-band celestial reference frame.

Key words: astrometry – reference systems – surveys

1. Introduction

The China Space Station Telescope (CSST) is a major science project of the China Manned Space Program (Su & Cui 2014), which is designed for extensive sky survey missions, featuring exceptional performance in both a wide field of view and high image quality. The telescope is equipped with several observation instruments, including a multi-color imaging and slitless spectrum survey module, a multi-channel imaging device, an integral field spectrograph, an exoplanet imaging coronagraph, and a high-sensitivity terahertz module. This series of observation instruments enables CSST to conduct a wide range of detailed observational studies of target celestial objects, promising breakthroughs in multiple astronomical research areas (Cao et al. 2018; Gong et al. 2019).

The primary mission of CSST is to conduct a comprehensive sky survey involving multi-color imaging and slitless spectrum observations, covering a total sky area of approximately 17,500 square degrees with a focus on medium to high galactic latitudes and ecliptic latitudes. The multi-color imaging detectors encompass seven wavelength bands, namely near-ultraviolet (NUV), u, g, r, i, z, and y-bands, among which the first six bands span a total wavelength range from 255 to 1000 nm. Each band has two or four CCDs and every CCD covers a sky area of 0.04 square degrees. In a typical observation with a 150 s exposure, the multi-color imaging detectors can achieve remarkably high limiting magnitudes of about 26 mag in the g-band detectors and approximately 25.5 mag in the other six bands.

In addition to its high limiting magnitude and wide wavelength coverage, CSST also has high astrometric precision and the position uncertainty is about 10 mas at magnitude 25 in the g-band (Fu et al. 2023). This makes CSST an instrument with the potential for valuable contributions to developing the celestial reference frame. Note that establishing a fundamental reference frame solely based on CSST observations is unfeasible due to its observation mode, therefore the future CSST data should be understood as an extension of current reference frames, particularly of the Gaia celestial reference frame (Gaia-CRF), which aligns well with CSST's wavelength coverage. The Gaia celestial reference frame 3 (Gaia-CRF3,

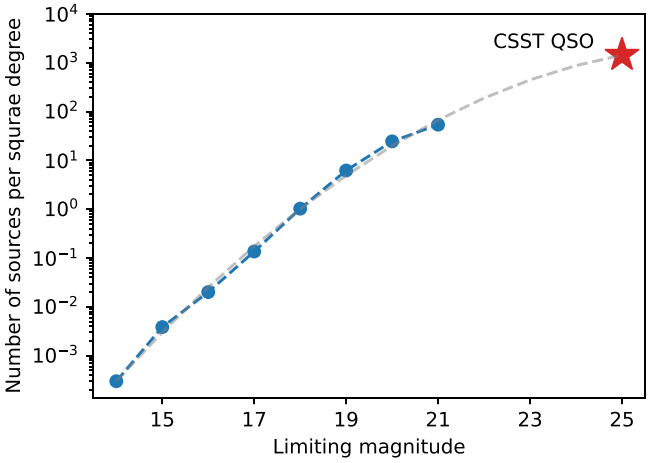

Figure 1. Growth of Gaia QSO-like object density in the CSST sky survey region as a function of Gaia *G*-magnitude. The gray dashed line is a logarithmic quadratic fitting of the Gaia density distribution and the red star represents the predicted density of the CSST sky survey at the faint end.

Gaia Collaboration et al. 2022a) is the latest version of Gaia-CRF. It was adopted as the optical realization of the International Celestial Reference System (ICRS) by the International Astronomical Union (IAU). The Gaia-CRF3 is defined by the positions and proper motions of approximately 1.6 million extragalactic sources in the third data release of Gaia (Gaia DR3, Gaia Collaboration et al. 2022b). The blue points in Figure 1 show the growth of the average Gaia DR3 quasi-stellar object (QSO)-like source density in the CSST sky area against Gaia *G* magnitude. At the limiting magnitude of 21, the density is approximately 50 per square degree. As the logarithm of the source density can be well fitted by a quadratic function (the gray dashed line), the extrapolated QSO-like source density in the CSST sky area at a limiting magnitude of 25.5 mag is expected to be approximately 1500 per square degree. This implies that CSST observations have the potential to substantially increase the source density in the current optical celestial reference frame. Moreover, CSST's high-precision observations in the Near-Infrared (NIR) and NUV bands further underscore its potential to broaden Gaia-CRF3 to a wider wavelength coverage.

In this paper, we compared the CSST sky survey and the Gaia-CRF3 to evaluate the potential astrometric performance of CSST to extend the Gaia-CRF3. Section 2 introduces the main methods used in our work. Then, we estimate the orientation precision of the CSST frame in Section 3. In Section 4, the CSST sky survey strategy, along with Gaia data, is used to evaluate the offsets between the prospective CSST celestial reference frame (CSST-CRF) and the current Gaia-CRF3. Section 5 provides a concise evaluation of CSST's performance in constructing multi-band reference frames and the conclusion is presented in Section 6.

2. The Vector Spherical Harmonics Fit

The main method used in our work to study the systematic differences between the two catalogs is the Vector Spherical Harmonics (VSH) developed by Mignard & Klioner (2012). In this method, the position differences of a set of common sources in two catalogs can be described by a vector field on a sphere:

$$\boldsymbol{y}(\alpha,\,\delta) = \sum_{l=1}^{\infty}\sum_{m=-l}^{l}(t_{lm}\boldsymbol{T}_{lm} + s_{lm}\boldsymbol{S}_{lm}). \tag{1}$$

Here, $(\alpha,\ \delta)$ are the equatorial coordinates of the sources, $\boldsymbol{y}(\alpha,\,\delta) = (\Delta\alpha\cos\delta,\ \Delta\delta) = [(\alpha_1 - \alpha_2)\cos\delta,\ \delta_1 - \delta_2]$ is the position differences, $\boldsymbol{T}_{lm}$ and $\boldsymbol{S}_{lm}$ are a series of orthogonal toroidal and spheroidal functions of VSH, and t_{lm} and s_{lm} are the coefficients. Based on this orthogonal decomposition, one can estimate the coefficients $\boldsymbol{x} = (t_{lm},\ s_{lm})$, which represent the systematic differences of two frames, through a least square fitting:

$$\boldsymbol{A}\boldsymbol{x} = \boldsymbol{y}, \tag{2}$$

$$\boldsymbol{x} = (\boldsymbol{A}^T\boldsymbol{W}\boldsymbol{A})^{-1}\cdot(\boldsymbol{A}^T\boldsymbol{W}\boldsymbol{y}), \tag{3}$$

where $\boldsymbol{A}$ is the matrix representing the VSH expansions and $\boldsymbol{W}$ is the weighted matrix. To compare the QSO reference frames like Gaia-CRF3 and future CSST-CRF, it is sufficient to use a VSH fitting of orders $l \leqslant 2$, where the first-order VSH coefficients describe the rotation and glide state of the frame and the second-order coefficients can be related to the gravity waves (Mignard & Klioner 2012). However, due to the lack of sufficient data to analyze the impact of factors such as gravitational waves on the Gaia-CRF3 and CSST-CRF alignment, the second-order coefficients were not considered in this work. We only used the first-order VSH fitting to study the rotation and glide between the two frames. The first-order VSH decomposition of position differences $(\Delta\alpha\cos\delta,\ \Delta\delta)$ is described as follows (Mignard & Klioner 2012):

$$\begin{aligned}\Delta\alpha\cos\delta = {} & R_1\cos\alpha\sin\delta + R_2\sin\alpha\sin\delta \\ & - R_3\cos\delta - G_1\sin\alpha + G_2\cos\alpha,\end{aligned} \tag{4}$$

$$\begin{aligned}\Delta\delta = {} & -R_1\sin\alpha + R_2\cos\alpha - G_1\cos\alpha\sin\delta \\ & - G_2\sin\alpha\sin\delta + G_3\cos\delta.\end{aligned} \tag{5}$$

Where $(R_1,\ R_2,\ R_3)$ are the rotation terms and $(G_1,\ G_2,\ G_3)$ are the glide terms. As a result, the estimated coefficients $\boldsymbol{x}$ is $(R_1,\ R_2,\ R_3,\ G_1,\ G_2,\ G_3)$.

In our fit, the position differences were weighted by the inverse of the sum of the squared position uncertainties in the two catalogs. Consequently, the weighted matrix $\boldsymbol{W}$ is defined

as:

$$\begin{aligned} \boldsymbol{W} &= \mathrm{COV}^{-1}(\Delta\alpha\cos\delta,\ \Delta\delta) \\ &= \begin{pmatrix} \sigma^2_{\alpha^*,1} + \sigma^2_{\alpha^*,2} & \rho_1\sigma_{\alpha^*,1}\sigma_{\delta,1} + \rho_2\sigma_{\alpha^*,2}\sigma_{\delta,2} \\ \rho_1\sigma_{\alpha^*,1}\sigma_{\delta,1} + \rho_2\sigma_{\alpha^*,2}\sigma_{\delta,2} & \sigma^2_{\delta,1} + \sigma^2_{\delta,2} \end{pmatrix}^{-1} \end{aligned} \tag{6}$$

where σ_{α^*} and σ_δ are the position uncertainties and ρ is the correlation coefficient. The formal uncertainties $\sigma_{\boldsymbol{x}}$ for the estimated results are obtained as the square root of the diagonal elements of $(\boldsymbol{A}^T\boldsymbol{W}\boldsymbol{A})^{-1}$. Additionally, the covariance matrix of $\boldsymbol{x}$, denoted as $\boldsymbol{\Sigma}$, is defined as $(\boldsymbol{A}^T\boldsymbol{W}\boldsymbol{A})^{-1}$.

3. Orientation Precision of the CSST-CRF

To make sure that the CSST-CRF is a useful extension of the current reference frame, it must be consistent with the Gaia-CRF3 in a global sense. A way to achieve this consistent alignment is to correct the rotation and glide between the CSST-CRF and Gaia-CRF3 in CSST positions. Since the rotation and glide estimated from the VSH fitting come with formal uncertainties, the corrected values are not strictly equal to the true orientation offset but are distributed around it, typically following a normal distribution. Smaller formal uncertainties in the estimated orientation offsets imply a higher consistency between the corrected values and the true offset. Equation (6) indicates that the uncertainties of the estimated orientation offsets are affected by the orientation accuracies of both CSST and Gaia reference frames. Therefore, achieving a consistent alignment requires that CSST has a high orientation precision, preferably comparable to that of Gaia-CRF3 if possible.

In this work, we evaluate the orientation uncertainty of the CSST-CRF by using the covariance matrix $\boldsymbol{\Sigma}$ derived from the first-order VSH fitting. As explained in Section 2, $\boldsymbol{W}^{-1}$ represents the sum of the covariance matrices for both Gaia and CSST coordinates. Consequently, $\boldsymbol{\Sigma}$ can be interpreted as the sum of the squared orientation uncertainties of the two reference frames. When considering only CSST source position uncertainties in the fit, i.e., $\boldsymbol{W}^{-1}_{\mathrm{CSST}} = \mathrm{COV}(\alpha_{\mathrm{CSST}}, \delta_{\mathrm{CSST}})$, we can determine the orientation uncertainty of the CSST-CRF from the corresponding $\boldsymbol{\Sigma} = (\boldsymbol{A}^T\boldsymbol{W}_{\mathrm{CSST}}\boldsymbol{A})^{-1}$. However, the complete matrix $\boldsymbol{\Sigma}$ contains 36 elements including both variance and covariance, which do not directly reflect the uncertainty. Here, the parameter $\bar{\sigma}$, serving as the geometric average of uncertainty, is used as a simplified representation in place of the complete matrix $\boldsymbol{\Sigma}$. Considering that the matrix $\boldsymbol{\Sigma}$ describes a six-dimensional error ellipsoid in the parameter space whose determinant ($|\boldsymbol{\Sigma}|$) is proportional to the square of the volume of the ellipsoid, the parameter $\bar{\sigma} = |\boldsymbol{\Sigma}|^{\frac{1}{12}}$ is the geometric average of the radius of the ellipsoid. Moreover, since the determinant of $|\boldsymbol{\Sigma}|$ is independent of the choice of coordinates, the parameter $\bar{\sigma}$ stays the same when another set of orthogonal rotation and glide axes are used (e.g., ecliptic coordinate). Therefore, using the geometric average of uncertainty $\bar{\sigma}$ to describe the orientation precision of the CSST reference frame is a suitable choice.

The calculation of $\boldsymbol{\Sigma}$ involves both matrices $\boldsymbol{A}$ and $\boldsymbol{W}$. Since the elements in matrix $\boldsymbol{A}$ are functions of the position (α, δ) and the elements in $\boldsymbol{W}$ are functions of the position errors, the position information of CSST sources is necessary for the calculation. We performed a simulation involving a series of extragalactic sources within the CSST-observed sky area, covering a magnitude range from 18 to 25 mag. The density of sources follows the distribution illustrated in Figure 1 which results in a simulated data set of about 22 million sources. Then, we used the uncertainty-magnitude relation of the Pan-STARRS1 (PS1, Chambers et al. 2016) sources in the g band to extrapolate the position error of the simulated CSST sources. The selection of PS1 is primarily based on two reasons. First, Pan-STARRS exhibits a similar observation mode to CSST, and has a very high accuracy of a few milliarcseconds. Second, PS1 achieves a limiting magnitude of about 23 mag, helping the extrapolation of CSST position uncertainty at the faint edge. As a result, the position uncertainty and magnitude distribution of the PS1 sources and the simulated sources are shown in Figure 2 using the blue and red points, respectively. Additionally, Gaia-CRF3 sources represented by gray points are also drawn for comparison.

Here, we divided the simulated sources into two groups based on their g magnitudes: those brighter than 21 mag (Gaia magnitude region) and those fainter than 21 mag, representing the bright and faint CSST frames, respectively. The corresponding estimated precisions for these two groups are denoted as $\bar{\sigma}_b$ and $\bar{\sigma}_f$, where the subscripts b and f represent bright and faint, respectively. Because the limitation of the Gaia observation is about 21 mag, only the bright CSST sources are used to calculate the orientation offset CSST-CRF and Gaia-CRF3. Consequently, the uncertainty in the orientation offset is influenced by $\bar{\sigma}_b$ but not by the precision of the entire CSST frame. In the bright group, including about 1 million sources, the calculated $\bar{\sigma}_b$ is about 11 μas. Note that the value and uncertainty of orientation offset between the Gaia-CRF3 and ICRF3 are about several microarcsecond (Gaia Collaboration et al. 2022a), this slightly larger uncertainty of CSST does not significantly affect the alignment to Gaia-CRF3. Due to the high density of simulated CSST sources at the faint edge, the estimated $\bar{\sigma}_f$ is only about 7 μas. If there is no systematic bias between the bright and faint CSST frames, the faint frame will also align to the Gaia-CRF3 at the level of tens of μas, allowing future faint reference frames to connect to Gaia-CRF3 via CSST.

However, it is important to note that our simulation of CSST position uncertainties is oversimplified and conservative. Since Pan-STARRS is a ground survey while CSST is a space telescope, the primary sources of uncertainty in the two

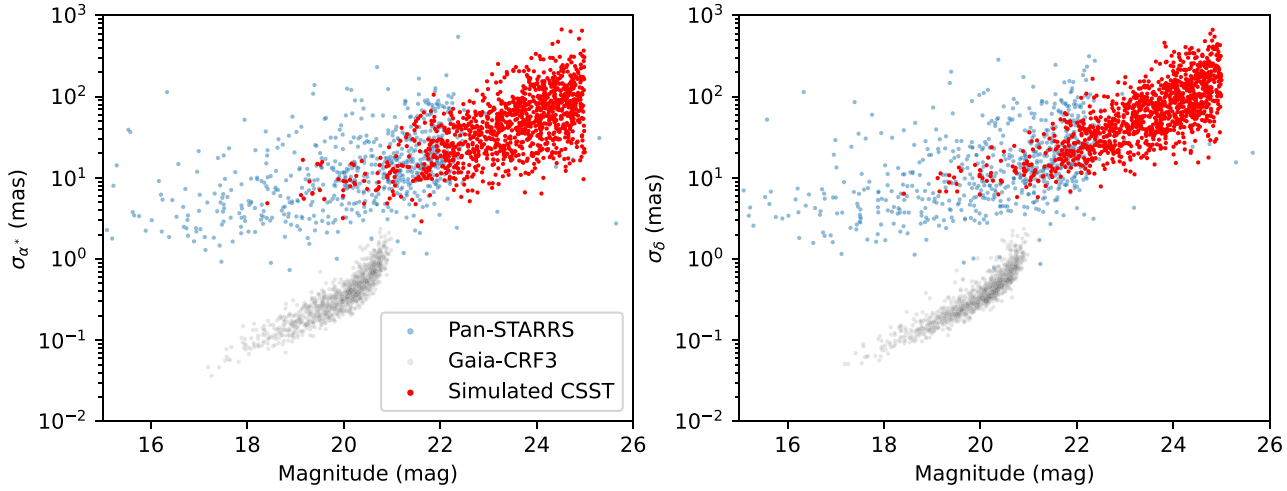

Figure 2. Position uncertainty and magnitude distribution of the Pan-STARRS1 sources (blue), Gaia-CRF3 sources (gray), and simulated CSST extragalactic sources (red). The magnitude of these three groups of sources are the Pan-STARRS g band, Gaia G band, and CSST g band, respectively.

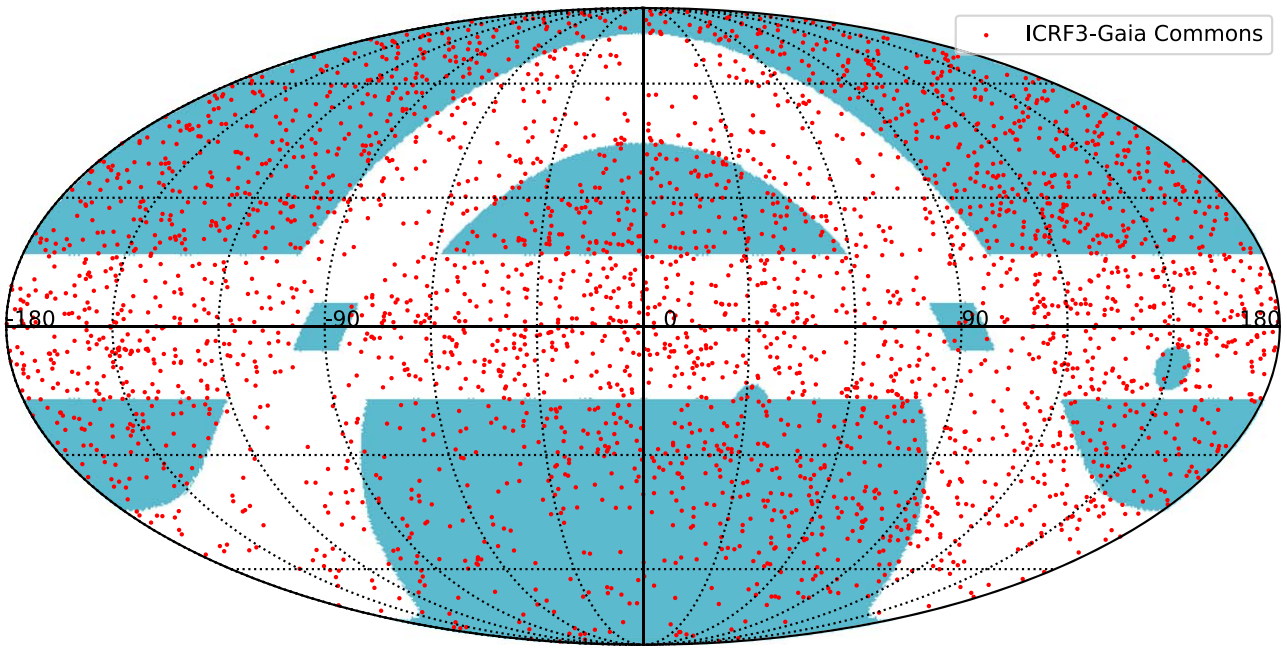

Figure 3. The covered sky area in the CSST sky survey (blue area) and the distribution of the ICRF3-Gaia CRF3 common sources (red points). All positions are in ecliptic coordinates.

observations differ. Moreover, our estimation only accounted for random error. In contrast, other optical catalogs, when compared to Gaia, demonstrate systematic offsets ranging from several mas to tens of mas (Kozhurina-Platais et al. 2018; Shi et al. 2019; Peng et al. 2023). It is expected that the alignment of future CSST-CRF and Gaia-CRF will primarily be influenced by systematic factors.

4. Systematic Effect of the Sky Area Selection of CSST

The CSST sky survey mainly focuses on deep and ultra-deep field observations which avoid regions with high stellar density in, or close to the Galactic plane ($|b| < 15°$). Furthermore, to mitigate the effects of solar interference, the low ecliptic latitude area ($|\beta| < 20°$) is also avoided. As shown in the blue part of Figure 3, the area of observed sky area is about 17,500

square degrees, less than half of the whole sky. As a result, the Gaia reference source used in CSST is a subset of Gaia-CRF3 (hereafter we refer to this subset of the Gaia-CRF3 as Gaia-CRF3′). Considering that the observation accuracy of sources is not uniform across the entire sky (Figure 8 in Gaia Collaboration et al. 2022b) in Gaia, the non-spherically symmetrically distributed area selected in Figure 3 may result in a systematic bias between Gaia-CRF3′ and Gaia-CRF3, and this bias will further impact the alignment between CSST-CRF and Gaia-CRF3.

4.1. Orientation Offset between the Gaia-CRF3′ and Gaia-CRF3

Because the data in Gaia-CRF3′ and Gaia-CRF3 both come from the third Gaia Data Release (Gaia DR3, Gaia Collaboration et al. 2022b), the method of using the position differences of the common source of two catalogs to estimate the orientation offset is infeasible. An alternative method is to compare Gaia-CRF3′ and Gaia-CRF3 with the aid of an intermediate celestial reference frame: the two reference frames are first compared with the intermediate frame independently, then the orientation offsets between Gaia-CRF3′ and Gaia-CRF3 can be derived from comparison of the results in the first step. A straightforward choice of the intermediate reference frame is the third International Celestial Reference Frame (ICRF3, Charlot et al. 2020) observed in the S/X band for the following reasons:

1. The ICRF3 is the fundamental realization of the ICRS in the radio domain. It is one of the most accurate celestial reference frames, achieving the position uncertainty of about several sub-mas.
2. The ICRF3 S/X catalog contains 4536 extragalactic sources, of which 3142 have counterparts in the Gaia-CRF3 catalog. As shown in Figure 3, the common sources are almost uniformly distributed in the sky, ensuring that there are enough sources in the alignment between Gaia-CRF3/Gaia-CRF3′ and ICRF3.
3. The ICRF3 and Gaia references are independent which helps us to understand the systematic effects of Gaia-CRF3 or Gaia-CRF3′.

The matched results of the Gaia-CRF3 and the ICRF3 S/X are obtained from Gaia Archive,[3] and the ICRF3 S/X data are downloaded from the IERS ICRS center.[4]

The comparison between the Gaia reference frame (either the complete one or the portion in the CSST observation area) and ICRF3 S/X follows the least squares fit of first-order VSH decomposition as described in Equations (4) and (5). Before the fit, The ICRF3 source positions are propagated from the ICRF3 epoch (J2015.0) to the Gaia-CRF3 epoch (J2016.0) using Equations (6) and (7) in Charlot et al. (2020) for the correction of the galactic aberration. The position differences $\boldsymbol{y}$ are then calculated in the sense of [ICRF3−Gaia]. To mitigate the impact of individual large values in $\boldsymbol{y}$, the outliers having large normalized angular separation $X > 4.01$ (X is defined in Equation (7)) are removed before fitting

$$X = \sqrt{\boldsymbol{y}^T \cdot \mathrm{COV}^{-1}(\Delta\alpha\cos\delta, \Delta\delta) \cdot \boldsymbol{y}}\,. \quad (7)$$

Assuming that the position differences are introduced by random errors only, the normalized angular separation X should satisfy the Rayleigh distribution. For a sample of 3142 common sources, the expected number of sources with normalized angular separation larger than 4.01 is less than 1, so the threshold for rejecting outliers is set to 4.01. The final sample used in comparison contains 2633 sources, of which 1414 are located in the CSST observation area (i.e., $b > 15°$ and $\beta > 20°$). The distribution of the normalized separation of the ICRF3−Gaia common sources is displayed in Figure 4.

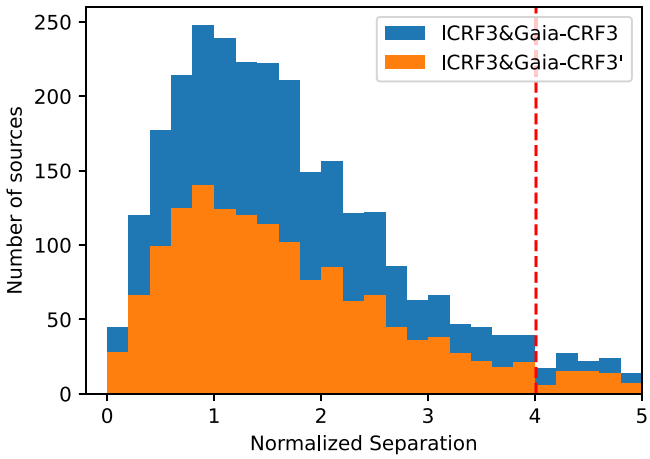

Figure 4. Histograms of the normalized angular separations between the ICRF3 S/X and Gaia-CRF3 for the 3142 common sources (blue) and the 1696 sources in the CSST observed region (orange). The red line is the threshold for the rejection and the outliers of these two samples are 509 and 282, respectively.

Table 1 presents the rotation and glide values between Gaia-CRF3 and ICRF3, as well as between Gaia-CRF3′ and ICRF3. All rotation and glide terms in both comparisons are less than 20 μas. Except for the G_3 term, the other estimated results for Gaia-CRF3′ are consistent with those of Gaia-CRF3 within the uncertainties. The last row is the difference between the two fitted results in the form of the Gaia-CRF3 fit minus the Gaia-CRF3′ fit which may be used to reflect the orientation bias between the Gaia-CRF3′ and Gaia-CRF3. From the table, it is observed that the rotation and glide between these two frames are comparable to the difference between Gaia-CRF3 and ICRF3 S/X. Given that the CSST observation is directly tied to Gaia-CRF3′, the bias between the Gaia-CRF3′ and Gaia-CRF3 is found to exert only slight influence on the alignment between

[3] https://gea.esac.esa.int/archive/
[4] https://hpiers.obspm.fr/icrs-pc/newwww/icrf/index.php

Table 1
Rotation and Glide Terms of the Transformations between ICRF3 S/X and the Two Frames (Gaia-CRF3 and Gaia-CRF3′), Plus the Difference of the Two Transformations Displayed in the Last Row

Reference Frame	Rotation Terms (μas)				Glide Terms (μas)			
	R_1	R_2	R_3	$\|R\|$	G_1	G_2	G_3	$\|G\|$
Gaia-CRF3	-1.0 ± 5.4	-8.8 ± 5.5	0.8 ± 4.6	8.9	12.3 ± 5.5	6.0 ± 5.1	-3.2 ± 4.9	14.1
Gaia-CRF3′	-1.7 ± 7.3	0.8 ± 7.4	-2.5 ± 6.5	3.2	12.7 ± 7.6	3.5 ± 6.8	-19.5 ± 7.0	23.5
$\Delta R(G)$	0.7 ± 9.1	-9.5 ± 9.2	3.3 ± 8.0	10.1	-0.4 ± 9.3	2.5 ± 8.5	16.3 ± 8.5	16.5

CSST-CRF and Gaia-CRF3, as well as on the extension to the Gaia-CRF3.

4.2. Glide and Residual Spin of the Gaia-CRF3′

The Gaia-CRF3 is established based on the positions of approximately 1.6 million QSO-like objects. In addition to precise source positions, the proper motions and parallax are also available for these extragalactic sources. Although insignificant, the proper motions of these sources introduce a subtle glide rate and spin in the Gaia-CRF3. The dominant factor contributing to the global glide rate in Gaia-CRF3 is the Galactic aberration (GA) effect, which leads to a glide vector of about 5.05 μas yr^{-1} (Gaia Collaboration et al. 2021) pointing to the Galactic center. The presence of residual spin is related to differences between the sources used in the frame rotator and those comprised in the Gaia-CRF3. Here, the frame rotator is a group of extragalactic sources used to estimate and correct the orientation and spin parameters in Gaia astrometric solution. Because the spin is sensitive to the selection of QSO-like sources, these differences between the rotator and CRF3 sources result in a residual spin of about 4 μas yr^{-1} in the Gaia-CRF3 (Gaia Collaboration et al. 2022a).

Since the Gaia-CRF3′ is a subset of the Gaia-CRF3 selected by the CSST sky survey region, the residual spin estimated from the proper motion of Gaia-CRF3′ sources may exhibit differences due to the sensitivity. Additionally, the estimation of the global glide rate may also be sensitive to source selection, resulting in potential variations between the Galactic aberration effect estimated in Gaia-CRF3′ and that in Gaia-CRF3. These discrepancies in spin and glide rate could subsequently impact the alignment between CSST-CRF and Gaia-CRF3. In light of this concern, we estimated the spin and glide rate of Gaia-CRF3′ and compared it to that of Gaia-CRF3. In this work, we applied first-order VSH to fit the proper motions of three groups of sources: Gaia-CRF3′, the full Gaia-CRF3, and all five-parameter QSO-like sources in Gaia-CRF3 (hereafter refer as Gaia-CRF3$_{5p}$). The last group is used to check whether our calculation of the GA effect is consistent with the result of Gaia Collaboration et al. (2021). The fitted rotation and glide from proper motions (Figure 5) indicate that the glide rates in all three cases reflect transformation introduced by the GA effect. The differences between any two cases are smaller than their corresponding uncertainties. This suggests that the incomplete sky area of Gaia-CRF3′ does not contribute extra glide of the CSST reference frame. In terms of global spin, only $\dot{R}_1$ term of Gaia-CRF3$_{5p}$ is approximately 1 μas yr^{-1} smaller than the other two cases. The differences in total spin and glide terms between the Gaia-CRF3′ and Gaia-CRF3 are around 0.5 and 0.3 μas yr^{-1}, respectively. These differential spin and glide can be neglected in the future study of the CSST reference frame.

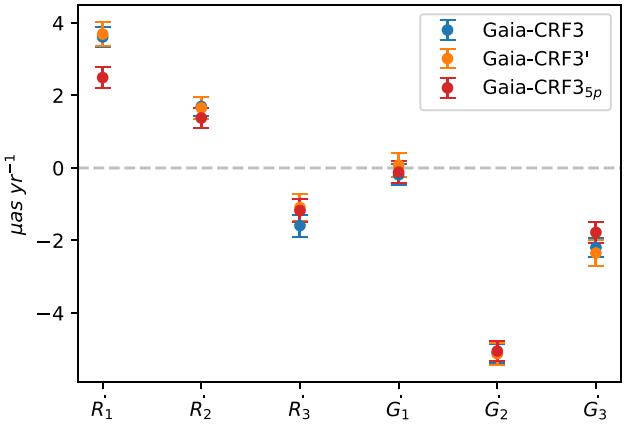

Figure 5. Spin and glide rate of the Gaia-CRF3, the Gaia-CRF3′, and the GaiaCRF3$_{5p}$.

5. CSST and Multi-band Reference Frame

To realize a fully integrated multi-band celestial reference frame, incorporating positions in both radio and optical bands and ensuring their consistency over the various bands, is a key objective of the IAU. In 2021, the adoption of the ICRF3 and Gaia-CRF3 as the fundamental realization of the ICRS for the radio and optical domains[5] marked the initial phase of the multi-band celestial reference frame initiative. To attain this objective, improvement of accuracy in all-sky observations across these spectral bands is necessary. The CSST sky survey, covering both NIR and NUV observations, holds promise as a valuable contributor. Current prominent catalogs in the infrared band include 2MASS (Skrutskie et al. 2006), WISE series

[5] https://www.iau.org/static/archives/announcements/pdf/ann21040c.pdf

Table 2
The Basic Information of the CSST Sky Survey and the Current Popular NIR and NUV Catalogs

Catalogs	Wavelength (μm)	N_{band}	Sky-coverage (square deg)	$N_{sources}$	Reference Frame	References
CSST	0.25–1.7	7	17,500		Gaia-CRF	
2MASS	1–3	3	full-sky	0.5 billion	Tycho-2	Skrutskie et al. (2006)
WISE	3–30	4	full-sky	0.6 billion	Tycho-2	Cutri et al. (2012)
PS1	0.4–1.5	5	30,900	1.9 billion	Gaia-CRF	Chambers et al. (2016)
GALEX	0.13–0.28	2	21,435	65 million	Tycho-2	Bianchi et al. (2011)

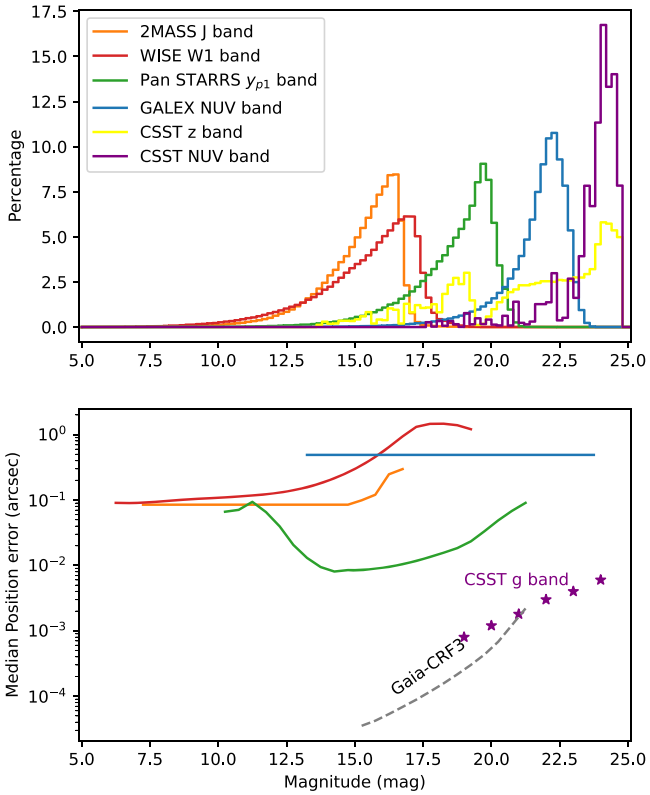

Figure 6. Upper panel: magnitude distribution of the sources in different catalogs. The distribution of the CSST is derived from the CSST Cycle 6 simulation (https://csst-tb.bao.ac.cn/code/csst_sim/csst-simulation). Bottom panel: position accuracy–magnitude relation of different catalogs, as well as the predicted accuracy of CSST (purple stars; Fu et al. 2023).

(Cutri et al. 2012, 2021; Schlafly et al. 2019; Marocco et al. 2021), and Pan-STARRS1 (Chambers et al. 2016), while the ultraviolet band is represented by the GALEX Bianchi et al. (2011). Statistical information of these catalogs, alongside projections for the future CSST sky survey, are presented in Table 2. All catalogs present source positions in the ICRS: the reference catalog for 2MASS, WISE, and GALEX is the Tycho-2 catalog, and the PS1 and CSST use the Gaia-CRF as reference catalog.

We compare the potential CSST catalog relative to existing catalogs from their limiting magnitude and observation accuracy. The magnitude distribution plotted in the upper panel of Figure 6 reveals that observations in the NIR band from popular catalogs are predominantly brighter than 20 mag, whereas CSST's z-band observations significantly extend into the fainter range of NIR observations. A similar situation can be seen in the NUV band, as visible in the distribution in the GALEX NUV band and CSST NUV band. Due to the increasing source density with magnitude, the CSST sky survey is poised to significantly enhance the density of the current celestial reference frame. The bottom panel in Figure 6 illustrates the position accuracy of four infrared or ultraviolet catalogs, Gaia-CRF3, and the anticipated CSST sky survey (Fu et al. 2023). Besides the CSST and Gaia-CRF3, PS1 achieves the highest accuracy of about 10 mas. However, the typical position uncertainty of Gaia-CRF3 sources, ranging from 1 to 2 mas, is an order of magnitude better than PS1. Existing observations fall short of realizing an infrared or ultraviolet frame comparable to ICRF3. The ideal position accuracy of CSST, represented by the purple stars in Figure 6 (bottom panel), indicates a formal error of about 10 mas at magnitude 24, comparable to Gaia. Consequently, the inclusion of CSST will contribute significantly to establishing the NIR and NUV reference frames in the future.

6. Summary

This study introduces the upcoming China Space Station Telescope and evaluates the performance of the CSST-CRF, the celestial reference frame based on the CSST multi-band sky survey. Given its wide wavelength coverage, deep field observations, and high-accuracy measurement, the CSST-CRF will be able to significantly extend the current Gaia-CRF3. According to the strategy and simulation of the CSST sky survey, we estimated the potential performance of the CSST-CRF.

First, we evaluated CSST's global orientation precision by calculating the covariance matrix. Based on the density-magnitude relationship of Gaia-CRF3 sources, we generated about 22 million extragalactic sources uniformly distributed in the CSST sky survey region, spanning magnitudes from 18 to 25 mag. The position uncertainties of these sources were also simulated according to the uncertainty-magnitude relation of the Pan-STARRS1 sources. The covariance matrix $\mathbf{\Sigma}$ of

orientation offset was derived from the least square fitting of the VSH, and $\bar{\sigma} = |\mathbf{\Sigma}|^{\frac{1}{12}}$ was used to describe the precision of the CSST frame. Considering the limiting magnitude of Gaia, we divided the simulated sources into two groups taking $g = 21$ mag as the threshold. The orientation uncertainty of the CSST extragalactic frame at the bright edge ($g < 21$ mag) is about 11 μas, and that at the faint edge ($g > 21$ mag) is about 7 μas. These uncertainties are not dominant when compared to the intrinsic offset between the Gaia-CRF3 and ICRF3.

Second, we discussed the systematic effect of incomplete coverage of the CSST sky area on the extension of the Gaia-CRF3. Due to limitations in sky coverage, CSST aligns with Gaia-CRF3′ (the subset of Gaia-CRF3 in the CSST-observed region) rather than the complete Gaia-CRF3. Using the ICRF3 S/X band as an intermediate reference frame, we estimated the orientation offset between the Gaia-CRF3 and the Gaia-CRF3′. The estimation showed that the rotation and glide offsets between the Gaia-CRF3 and the Gaia-CRF3′ are less than 20 μas, comparable to the offsets between Gaia-CRF3 and ICRF3 in our analysis. This suggests that the sky area selection introduces an insignificant systematic effect between the Gaia-CRF3 and Gaia-CRF3′. We also estimated the residual spin and glide rate of the Gaia-CRF3′ to investigate the influence of the sky selection. The fitted results for spin and glide rate of Gaia-CRF3′ are consistent with that of Gaia-CRF3. Consequently, the sky area selection in CSST does not significantly impact the CSST extension to Gaia-CRF3.

Finally, the contribution of CSST in the work of multi-band celestial reference frame is discussed through a comparison with current catalogs containing the observations in the NIR and NUV bands. In these two bands, CSST exhibits unparalleled accuracy and depth, uniquely possessing accuracy comparable to Gaia. The observations conducted by CSST are poised to significantly advance the establishment of a comprehensive multi-band reference frame.

Acknowledgments

This work is funded by the science research grants from the China Manned Space Project with NO.CMS-CSST-2021-A11 and NO. CMS-CSST-2021-B10. We also acknowledge the National Natural Science Foundation of China (NSFC) under grant No. 12373074.

References

Bianchi, L., Herald, J., Efremova, B., et al. 2011, Ap&SS, 335, 161
Cao, Y., Gong, Y., Meng, X.-M., et al. 2018, MNRAS, 480, 2178
Chambers, K. C., Magnier, E. A., Metcalfe, N., et al. 2016, arXiv:1612.05560
Charlot, P., Jacobs, C. S., Gordon, D., et al. 2020, A&A, 644, A159
Cutri, R. M., Wright, E. L., Conrow, T., et al. 2021, yCat, II/328
Cutri, R. M., Wright, E. L., Conrow, T., et al. 2012, yCat, II/311
Fu, Z.-S., Qi, Z.-X., Liao, S.-L., et al. 2023, FrASS, 10, 1146603
Gaia Collaboration, Klioner, S. A., Lindegren, L., et al. 2022a, A&A, 667, A148
Gaia Collaboration, Klioner, S. A., Mignard, F., et al. 2021, A&A, 649, A9
Gaia Collaboration, Vallenari, A., Brown, A. G. A., et al. 2022b, arXiv:2208.00211
Gong, Y., Liu, X., Cao, Y., et al. 2019, ApJ, 883, 203
Kozhurina-Platais, V., Grogin, N., & Sabbi, E. 2018, Accuracy of the HST Standard Astrometric Catalogs w.r.t. Gaia, Instrument Science Report ACS 2018-01, 17
Marocco, F., Eisenhardt, P. R. M., Fowler, J. W., et al. 2021, ApJS, 253, 8
Mignard, F., & Klioner, S. 2012, A&A, 547, A59
Peng, X., Qi, Z., Zhang, T., et al. 2023, AJ, 165, 172
Schlafly, E. F., Meisner, A. M., & Green, G. M. 2019, ApJS, 240, 30
Shi, Y. Y., Zhu, Z., Liu, N., et al. 2019, AJ, 157, 222
Skrutskie, M. F., Cutri, R. M., Stiening, R., et al. 2006, AJ, 131, 1163
Su, D.-Q., & Cui, X.-Q. 2014, RAA, 14, 1055